

***Ab initio* local stress and its application to Al (111) surfaces**Yoshinori Shiihara,^{1,*} Masanori Kohyama,² and Shoji Ishibashi¹¹*Research Institute for Computational Sciences (RICS), National Institute of Advanced Industrial Science and Technology (AIST), 1-1-1 Umezono, Tsukuba, Ibaraki 305-8568, Japan*²*Research Institute for Ubiquitous Energy Devices (UBIQEN), AIST, 1-8-31, Midorigaoka, Ikeda, Osaka 563-8577, Japan*
(Received 23 July 2009; revised manuscript received 11 January 2010; published 26 February 2010)

A practical way to calculate local quantum stress within the framework of stress density developed by Filippetti and Fiorentini [Phys. Rev. B **61**, 8433 (2000)] is proposed and applied to Al (111) surfaces. Through detailed analysis of the gauge-dependent term in the kinetic stress density derived from the kinetic-energy density, it has been shown that the local stress components can be uniquely obtained by defining appropriate local regions where the gauge-dependent term integrates to zero. In Al (111) surface-slab calculations implemented by the projector-augmented-wave method, we have observed Friedel-type oscillation of the layer-by-layer stress, which reveals clear correlation with charge redistribution at the surface.

DOI: [10.1103/PhysRevB.81.075441](https://doi.org/10.1103/PhysRevB.81.075441)

PACS number(s): 68.35.Gy, 71.15.-m, 68.47.De

I. INTRODUCTION

A material under strain shows different physical properties from those of the bulk equilibrium state. For example, a semiconductor under strain shows a larger or smaller band gap.¹⁻³ Correlation between strain and magnetic anisotropy^{4,5} or polarization^{6,7} in some materials is often quoted as another example. In a microscopic view, the change in the physical properties is attributed to the variations in electronic structure and atomic arrangement induced by strain. As the basic susceptibility for the strain, stress can be defined as the total-energy derivative with respect to strain. Because the stress is zero when the equilibrium structure is unstrained, the stress allows us to know whether the atomic structure is strained or not without the knowledge about the stable structure. Stress can be also utilized to know the effect of defected structures (e.g., surface and interface) on the bulk state. In recent studies, there have been growing interests in estimating local stress at surfaces, interfaces, and grain boundaries in view of experiment and simulation.⁸⁻¹² Such local stress can be also defined as the local contribution to the total-energy derivative with respect to strain.

In the long history of attempts at estimating quantum stress,¹³ the practical implementation of *ab initio* stress calculations was started by the works of Nielsen and Martin.^{14,15} They derived quantum total stress from the variation in density-functional total energy with respect to uniform strain of crystals or repeated cell systems. The total stress is a cell-averaged value and is frequently employed in cell-size relaxation in conventional *ab initio* calculations. Besides the importance of the total quantum stress, local quantum stress is also a remarkable concept to deal with defects, surfaces, or interfaces, for example, for which one has to analyze separate contributions to the total stress of the system from defected and bulk regions. Filippetti and Fiorentini¹⁶ proposed the concept of stress density and applied it to surface and interface problems. In analogy with the energy density proposed by Chetty and Martin,¹⁷ the stress density is defined as a stress-field tensor distributed in a unit cell and integrates to the total stress. They showed that

the stress density can appropriately express the stress state in the vicinity of surfaces or interfaces. Apart from the stress density defined by homogeneous strain of supercell configurations, more general stress-field tensors defined by the local balance relation or by inhomogeneous strain have been also proposed.¹⁸⁻²¹ Regardless of the definition of stress-field tensor, there is an intrinsic shortcoming in quantum stress-field tensor: it is nonuniqueness. For example, in the case of the stress density, any function which integrates to zero over the cell can be added to the stress density because the density is defined as an integrand which integrates to the total stress as in the case of the energy density. This means that the stress density can only be specified up to a gauge term, hence this problem is called as a gauge-dependent problem.^{21,22} All the quantum stress-field tensors proposed so far suffer this problem, which prevents one to use the tensor as a well-defined physical quantity. In order to average out the gauge dependency, a macroscopic averaging^{16,17,23} or an integration scheme²⁴ can be applied as in the same way applied to the energy density. However, it is difficult to define period lengths or partial regions in the case that the electronic structure or the atomic arrangement is largely changed from its bulk state. To apply the concept of the stress density or other stress-field tensors to the estimation of local stress in various complex systems, a robust scheme to average out the gauge-dependent term is required.

The purpose of this paper is to develop a practical way to calculate more reliable local quantum stress by using the stress density on the basis of plane-wave pseudopotential techniques.²⁵⁻²⁷ To this end, we propose a scheme to remove the effects of the gauge-dependent terms and related ambiguities. When considering that the stress density can be derived from the strain derivative of the integrated form of the energy density, it is natural to attribute the gauge dependence of the stress density to that of the energy density. Hence, we start off by specifying the gauge-dependent term in the energy density and particularly consider the nonuniqueness problem in the kinetic-energy contribution. The derived gauge-dependent term in the kinetic stress density has a similar form to the one proposed by Rogers and Rappe.²¹ We also observe that some ambiguities are contained in the nonlocal

pseudopotential and electrostatic terms while these are localized in the vicinity of the atomic cores. To obtain the definite local stress values, we define local regions partitioned in the supercell, where the gauge-dependent terms are integrated to be zero and the other ambiguities are averaged out.

In this study, the stress-density calculation is implemented by the projector-augmented-wave (PAW) method^{27,28} instead of the ultrasoft pseudopotential (USPP) method²⁶ employed by Filippetti and Fiorentini while the present scheme can be generally used in various pseudopotential methods. The PAW-based stress density was successfully applied to the investigation of the microscopic distributions of electric-field-induced stress in diamond/cBN superlattices.²⁹ In order to show the validity of the present scheme, we perform the layer-by-layer stress calculations of Al (111) surfaces, which are compared with previous theoretical results.³⁰⁻³² We found remarkable correlation between the stress distribution and the charge redistribution at the Al surface.

This paper is organized as follows. In Sec. II, the detailed formulation of the energy density and the stress density is analyzed and their gauge-dependent terms are specified. Then we describe the integration scheme to remove the gauge dependency and related ambiguities for the local stress calculations. In Sec. III, the present scheme is applied to the Al (111) surface.

II. SCHEMES

A. Local stress and gauge-dependent problem

In estimation of local stress in a certain atomic system, a stress-field tensor is required as a distributed quantity over the system. We employ the stress density proposed by Filippetti and Fiorentini.¹⁶ The stress density is defined as an integrand of the macroscopic stress proposed by Nielsen and Martin,¹⁴

$$\bar{\sigma}_{\alpha\beta} = \frac{1}{V} \int_V \tau_{\alpha\beta}(\mathbf{r}) d\mathbf{r}, \quad (1)$$

where V is the whole region of the supercell.³³ The macroscopic stress is defined as the variation in the total energy E_{tot} with respect to uniform strain of a repeated cell system as

$$\bar{\sigma}_{\alpha\beta} = \frac{1}{V} \frac{\partial E_{\text{tot}}}{\partial \varepsilon_{\alpha\beta}}. \quad (2)$$

Then the local stress can be defined as

$$\bar{\sigma}_{\alpha\beta}(i) = \frac{1}{V_i} \int_{V_i} \tau_{\alpha\beta}(\mathbf{r}) d\mathbf{r}, \quad (3)$$

where V_i is the i th partial region. Through Eqs. (2) and (3), the local stress is defined as the energy response of a partial region against a uniform strain tensor $\varepsilon_{\alpha\beta}$. On the other hand, the energy density is defined as an integrand of the total energy,¹⁷

$$E_{\text{tot}} = \int_V e_{\text{tot}}(\mathbf{r}) d\mathbf{r}. \quad (4)$$

Since the energy density and the stress density are defined as an integrand, an arbitrary function term (gauge-dependent term) which integrates to zero over the whole cell can be added to the densities. This arbitrariness is inevitable and prevents one from using the energy density or the stress density as a well-defined physical quantity. However, any function which integrates to zero may not be necessarily included in the energy and stress densities. In this study, we assume that the arbitrary function should be physically motivated.¹⁸

From Eqs. (1), (2), and (4), the stress density should be derived from the strain derivative of the integration form of the energy density. This derivation is performed by scaling procedure given in the works of Nielsen and Martin.^{14,15} Detailed procedure of the derivation is given for the kinetic and exchange-correlation components in Appendices A and B, as examples, where a specific form of each stress-density component can be obtained from the corresponding energy density component via the scaling procedure. Thus a gauge-dependent term in the stress density can be assumed to be originated from that in the energy density.

B. Gauge dependence of energy density

The total-energy density in the density-functional theory (DFT) of pseudopotential formalism is comprised of the following components:

$$e_{\text{tot}}(\mathbf{r}) = e_{\text{kin}}(\mathbf{r}) + e_{\text{es}}(\mathbf{r}) + e_{\text{nl}}(\mathbf{r}) + e_{\text{xc}}(\mathbf{r}), \quad (5)$$

where e_{kin} is the kinetic-energy density, e_{es} is the electrostatic energy density, e_{nl} is the nonlocal pseudopotential energy density related to pseudopotential methods, and e_{xc} is the exchange-correlation energy density. Here the form of each component is described basically according to Chetty and Martin.¹⁷

The kinetic-energy density e_{kin} can be defined in the following two expressions.³⁴ The symmetric form is

$$e_{\text{kin,S}}(\mathbf{r}) = \frac{1}{2} \sum_i f_i \nabla \psi_i^*(\mathbf{r}) \cdot \nabla \psi_i(\mathbf{r}) \quad (6)$$

and the asymmetric form is

$$e_{\text{kin,AS}}(\mathbf{r}) = -\frac{1}{2} \sum_i f_i \psi_i^*(\mathbf{r}) \nabla^2 \psi_i(\mathbf{r}), \quad (7)$$

where ψ_i is a valence wave function and f_i is an occupation number. Although both forms give the same kinetic-energy value when they are integrated over the whole cell, their distributions are distinctly different from each other. Yang *et al.*³⁵ discussed the uniqueness of the kinetic-energy density based on its asymptotic behavior at an infinite distance and proposed the following form as the kinetic-energy density:

$$e_{\text{kin}}(\mathbf{r}) = e_{\text{kin,S}}(\mathbf{r}) + \gamma \nabla^2 \rho_e(\mathbf{r}), \quad (8)$$

where ρ_e is the valence electron density and γ is an arbitrary constant. The derivation of Eq. (8) from Eqs. (6) and (7) is shown in Appendix A. When γ is $-1/4$, e_{kin} turns to be $e_{\text{kin,AS}}$. Since the Laplacian of the electron density integrates to zero, the Laplacian term is the gauge-dependent term. We employ Eq. (8) as the kinetic-energy density because the gauge-dependent term is explicitly included in this form.

The electrostatic energy density e_{es} represents electrostatic interactions among valence electrons and ions. In order to break the electrostatic energy density down into long-range and short-range parts, a fictitious ionic charge density ρ_{ion} is introduced as

$$\rho_{\text{ion}}(\mathbf{r}) = - \sum_{\mu} \frac{Z_{\mu}}{(\sqrt{\pi}\lambda_{\mu})^3} \exp\left[-\frac{|\mathbf{r} - \mathbf{R}_{\mu}|^2}{\lambda_{\mu}^2}\right], \quad (9)$$

where λ_{μ} represents a Gaussian width set for of an atom μ . For simplicity, the same value λ_c is employed for every atom. In the present study, the sign of the charge is positive for the electron and negative for the ionic core. A total charge ρ_{tot} is also defined by

$$\rho_{\text{tot}}(\mathbf{r}) = \rho_e(\mathbf{r}) + \rho_{\text{ion}}(\mathbf{r}). \quad (10)$$

For these charge densities, their corresponding electrostatic potentials, v_{tot} , v_e , and v_{ion} can be defined through the Poisson equation. By using these potentials, we define the electrostatic energy density as

$$\begin{aligned} e_{\text{es}}(\mathbf{r}) = & \frac{1}{8\pi} \nabla v_{\text{tot}}(\mathbf{r}) \cdot \nabla v_{\text{tot}}(\mathbf{r}) + v'_{\text{loc}}(\mathbf{r})\rho_e(\mathbf{r}) \\ & + \frac{1}{2} \sum_{\mu \neq \mu'} \delta(\mathbf{r} - \mathbf{R}_{\mu}) \frac{Z_{\mu}Z_{\mu'}}{|\mathbf{R}_{\mu} - \mathbf{R}_{\mu'}|} \\ & \times \left\{ \text{erfc}\left(\frac{|\mathbf{R}_{\mu} - \mathbf{R}_{\mu'}|}{\sqrt{2}\lambda_c}\right) \right\} - \frac{1}{\sqrt{2\pi}} \sum_{\mu} \delta(\mathbf{r} - \mathbf{R}_{\mu}) \frac{Z_{\mu}^2}{\lambda_{\mu}}, \end{aligned} \quad (11)$$

where v'_{loc} is a short-range local potential given by

$$v'_{\text{loc}}(\mathbf{r}) = v_{\text{loc}}(\mathbf{r}) - v_{\text{ion}}(\mathbf{r}). \quad (12)$$

The electrostatic interactions among valence electrons and ions are included in the first term of Eq. (11) as the interactions among valence electrons and the fictitious ionic charges of Eq. (9), and thus the second term is generated as the correction for the replacement of the local pseudopotentials v_{loc} by v_{ion} . The third term is an overlap sum and the fourth term represents self-interaction of the pseudoionic cores. These two terms are corrections for the replacement of the electrostatic interactions among ionic point charges by the interactions among the fictitious ionic charges in the first term of Eq. (11) and are described as distribution to each ionic core by using δ functions. As a result, only the first term of Eq. (11) is long ranged and the others are short

ranged. Mathematically there are two types of expressions for the electrostatic energy density as in the case of kinetic-energy density. The first is the Maxwell form expressed as a dot product of gradient vectors of electrostatic potential and the second is a form expressed as a product of electrostatic potential and its corresponding charge density.³⁶ Here we assume the Maxwell form is the unique expression because it can correctly represent the energy density in not only static problems but also dynamic problems.³⁶ In Eq. (11), only the first term has the Maxwell form and the others do not while this ambiguity will be settled because they are localized in atomic sites.

The nonlocal pseudopotential energy density e_{nl} is localized inside the atomic sphere and is described by using a δ function as

$$e_{\text{nl}}(\mathbf{r}) = \sum_{\mu} \delta(\mathbf{r} - \mathbf{R}_{\mu}) E_{\text{nl},\mu}, \quad (13)$$

where $E_{\text{nl},\mu}$ is the nonlocal pseudopotential energy per atom represented by using nonlocal operator $\hat{v}_{\text{nl},\mu}$ as

$$\begin{aligned} E_{\text{nl},\mu} = & \sum_i f_i \int \int \psi_i^*(\mathbf{r}') \hat{v}_{\text{nl},\mu}(\mathbf{r}' - \mathbf{R}_{\mu}, \mathbf{r}'' - \mathbf{R}_{\mu}) \\ & \times \psi_i(\mathbf{r}'') d\mathbf{r}' d\mathbf{r}''. \end{aligned} \quad (14)$$

The form of $E_{\text{nl},\mu}$ depends on the choice of pseudopotential schemes. The detailed form in the PAW scheme is given in Appendix C. Several ambiguous terms can appear in it concerning the kinetic and electrostatic energies while we need not to consider such ambiguity owing to its locality. Finally, the form of the exchange-correlation energy density e_{xc} depends on used functional forms of local-density approximation (LDA) or generalized gradient approximation (GGA). The definition problem of e_{xc} is identical to seeking for the exact exchange-correlation functional, which is beyond the aim of the present study. Hence we ignore the gauge-dependent problem in the exchange-correlation energy density.

C. Gauge dependence of stress density

The gauge-dependent term in the stress density is attributed to that in the energy density. In the preceding section, the gauge-dependent term is explicitly specified in the kinetic-energy density but not so in the other energy densities. The reason is summarized as follows. First, we can select the Maxwell energy density as the unique expression of the electrostatic energy density. Second, the gauge dependence on the localized energy densities such as nonlocal pseudopotential energy density can be removed by integration in each atomic site. And third, we do not deal with the gauge-dependent term in the exchange-correlation energy density. Here we show the expression of the stress density derived from the energy density and examine the gauge-dependent problem.

The stress density is comprised of the following components:³⁷

$$\tau_{\alpha\beta}(\mathbf{r}) = \tau_{\text{kin},\alpha\beta}(\mathbf{r}) + \tau_{\text{es},\alpha\beta}(\mathbf{r}) + \tau_{\text{nl},\alpha\beta}(\mathbf{r}) + \tau_{\text{xc},\alpha\beta}(\mathbf{r}), \quad (15)$$

where τ_{kin} is the kinetic stress density, τ_{es} is the electrostatic stress density, τ_{nl} is the nonlocal stress density related to the

pseudopotential methods, and τ_{xc} is the exchange-correlation stress density. The kinetic stress density τ_{kin} is derived from Eqs. (6) and (8) as

$$\tau_{\text{kin},\alpha\beta}(\mathbf{r}) = - \sum_i f_i \nabla_\alpha \psi_i(\mathbf{r}) \nabla_\beta \psi_i(\mathbf{r}) - 2\gamma \frac{\partial}{\partial r_\alpha} \frac{\partial \rho_e(\mathbf{r})}{\partial r_\beta}. \quad (16)$$

The detailed derivation is given in Appendix A. The second term of Eq. (16) is the gauge-dependent term of the kinetic stress density. The electrostatic stress density τ_{es} is derived from Eq. (11) as

$$\begin{aligned} \tau_{\text{es},\alpha\beta}(\mathbf{r}) = & -\delta_{\alpha\beta} \frac{1}{8\pi} \nabla v_{\text{tot}}(\mathbf{r}) \cdot \nabla v_{\text{tot}}(\mathbf{r}) + \frac{1}{4\pi} \nabla_\alpha v_{\text{tot}}(\mathbf{r}) \nabla_\beta v_{\text{tot}}(\mathbf{r}) + \left[\delta_{\alpha\beta} \rho_e(\mathbf{r}) + \frac{\partial \rho_e(\mathbf{r})}{\partial \varepsilon_{\alpha\beta}} \right] \cdot v_{\text{tot}}(\mathbf{r}) + \frac{\lambda_c^2}{4} [\nabla_\alpha \rho_{\text{ion}}(\mathbf{r}) \nabla_\beta v_{\text{tot}}(\mathbf{r}) \\ & + \nabla_\alpha v_{\text{tot}}(\mathbf{r}) \nabla_\beta \rho_{\text{ion}}(\mathbf{r})] + \delta_{\alpha\beta} v'_{\text{loc}}(\mathbf{r}) \rho_e(\mathbf{r}) + \frac{\partial \rho_e(\mathbf{r})}{\partial \varepsilon_{\alpha\beta}} v'_{\text{loc}}(\mathbf{r}) + \frac{\partial v'_{\text{loc}}(\mathbf{r})}{\partial \varepsilon_{\alpha\beta}} \rho_e(\mathbf{r}) - \sum_{\mu \neq \mu'} \delta(\mathbf{r} - \mathbf{R}_\mu) Z_\mu Z_{\mu'} (\mathbf{R}_\mu - \mathbf{R}_{\mu'})_\alpha (\mathbf{R}_\mu \\ & - \mathbf{R}_{\mu'})_\beta \times \left[\frac{1}{2|\mathbf{R}_\mu - \mathbf{R}_{\mu'}|^3} \text{erfc}\left(\frac{|\mathbf{R}_\mu - \mathbf{R}_{\mu'}|}{\sqrt{2}\lambda_c}\right) + \frac{1}{\sqrt{2}\pi\lambda_c |\mathbf{R}_\mu - \mathbf{R}_{\mu'}|^2} \exp\left(-\frac{|\mathbf{R}_\mu - \mathbf{R}_{\mu'}|^2}{2\lambda_c^2}\right) \right]. \end{aligned} \quad (17)$$

The first four terms on the right-hand side of Eq. (17) come from the first term on the right-hand side of Eq. (11). The fifth, sixth, and seventh terms come from the second term of Eq. (11). The last term is related to the overlap sum. The self-interaction term does not appear because the self-interaction energy does not change under uniform deformation. It should be noted that the terms which come from the short-range terms of the electrostatic energy density are concerned with the ambiguity while these are localized in the atomic sites as in the case of the electrostatic energy density.

The nonlocal pseudopotential term τ_{nl} is given as

$$\tau_{\text{nl},\alpha\beta}(\mathbf{r}) = \sum_\mu \delta(\mathbf{r} - \mathbf{R}_\mu) \frac{\partial}{\partial \varepsilon_{\alpha\beta}} E_{\text{nl},\mu}. \quad (18)$$

The practical form in the PAW method appears in Appendix C. This stress component is localized at the atomic sites. The exchange-correlation stress density τ_{xc} is given by

$$\tau_{\text{xc},\alpha\beta}(\mathbf{r}) = \delta_{\alpha\beta} e_{\text{xc}}(\mathbf{r}) + \frac{\partial e_{\text{xc}}}{\partial \rho_e} \frac{\partial \rho_e}{\partial \varepsilon_{\alpha\beta}} + \frac{\partial e_{\text{xc}}}{\partial \nabla \rho_e} \cdot \frac{\partial \nabla \rho_e}{\partial \varepsilon_{\alpha\beta}}. \quad (19)$$

Finally, the pressure distribution $p(\mathbf{r})$ can be also defined by using the stress density as

$$p(\mathbf{r}) = \frac{1}{3} \sum_{\alpha=1}^3 \tau_{\alpha\alpha}(\mathbf{r}). \quad (20)$$

The gauge-dependent term in the kinetic stress density described above is similar to the one proposed by Rogers and Rappe²¹ or Godfrey¹⁹ in spite of the difference in the formu-

lation. According to the analysis of Godfrey, the symmetric and asymmetric kinetic stress forms linked via the parameter γ exhaust the physically reasonable gauges. While Rogers and Rappe limit the range of parameter γ in Eq. (8) from 0 to $-1/4$, we do not limit the range of γ because any value of γ is acceptable according to the work of Yang *et al.*³⁵ As regards the electrostatic part of the stress field, two stress forms have been considered as physically reasonable possible gauges: the Maxwell stress^{14,38} and the form proposed by Kugler.^{19,39,40} Ziesche *et al.*⁴¹ attributed this ambiguity to that of the electromagnetic energy density. In the present study, the Maxwell stress density derived from the Maxwell energy density is taken to be the unique electrostatic stress density because the Maxwell energy density is assumed to be the unique one. This treatment of the electrostatic stress field coincides with the work by Rogers and Rappe. In our formulation of the stress density, ambiguous terms can be included in the electrostatic and nonlocal pseudopotential stress densities while this problem will be settled by the localization of these terms.

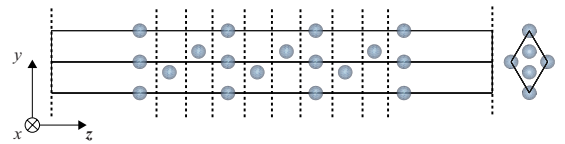


FIG. 1. (Color online) Slab model of the Al (111) surface consisting of ten atomic layers. Side view (left) and top view (right). Solid lines represent the boundaries of periodic supercells and vertical broken lines represent the partitioning planes for the local stress calculation.

D. Gauge-independent local stress

To remove the gauge-dependent term, we employ the integration scheme. The local stress should be uniquely obtained by integrating the stress density within a certain partial region where the gauge-dependent term integrates to zero. Here we show how to divide the whole cell into such partial regions. First, for such a partial region V_i , the gauge-dependent term in Eq. (16) should integrate to zero as

$$\sigma'_{\alpha\beta}(i) = \frac{1}{V_i} \int_{V_i} \frac{\partial}{\partial r_\alpha} \frac{\partial \rho_e(\mathbf{r})}{\partial r_\beta} d\mathbf{r} = 0. \quad (21)$$

The volume integral $\sigma'_{\alpha\beta}$ over an i th partial region can be transformed to the surface integral as

$$\sigma'_{\alpha\beta}(i) = \frac{1}{V_i} \int_{S_i} \frac{\partial \rho_e(\mathbf{r})}{\partial r_\beta} \mathbf{e}_\alpha \cdot \mathbf{n} dS = 0, \quad (22)$$

where \mathbf{e}_α is a unit vector codirectional with the α axis and \mathbf{n} is a surface normal. Thus the partial regions have to be partitioned by the boundaries satisfying the condition of Eq. (22). Second, such boundaries should be selected so that atomic cores are contained inside the partial regions due to the ambiguity problem in the electrostatic and nonlocal pseudopotential components. The ambiguity of the short-range terms other than those expressed by δ functions in the electrostatic stress density can be settled by localizing these terms at the atomic sites via a proper Gaussian width of the fictitious ionic charge density.

We apply the present scheme to surface-slab calculations. We deal with an Al (111) slab as shown in Fig. 1. The partitioning planes parallel to the surface plane (x - y plane) are set between the atomic layers (ALs), resulting in a one-dimensional problem. The local stress is defined in each partial region surrounded by the partitioning planes, which means that the macroscopic stress is decomposed into the layer-by-layer stress. In the present case, the integration scheme can be simplified because the conditions of Eq. (22) are automatically satisfied except for σ'_{zz} due to the periodicity on the x - y planes: only σ'_{zz} is gauge dependent in the layer-by-layer decomposition. The condition to make σ'_{zz} gauge-independent quantity turns to be

$$\int_{S_i} \frac{\partial \rho_e(\mathbf{r})}{\partial z} dx dy = \int_{S_{i+1}} \frac{\partial \rho_e(\mathbf{r})}{\partial z} dx dy, \quad (23)$$

where S_i and S_{i+1} indicate i th and $(i+1)$ th partitioning planes to satisfy the condition of the flux of the electron density.

E. Computational details

The present scheme was applied to the Al (111) surface using the PAW method^{27,28} with our in-house *ab initio* code QMAS (Quantum MAterials Simulator).²⁹ We use GGA (Ref. 42) for the exchange-correlation functional. Gaussian smearing method⁴³ with a width of 0.01 eV is employed to introduce partial occupancies. High numerical accuracy is required to obtain a well-converged stress value. The k -point mesh in the full Brillouin zone was $16 \times 16 \times 16$ for the fcc conventional cell and $32 \times 32 \times 2$ for the surface and bulk

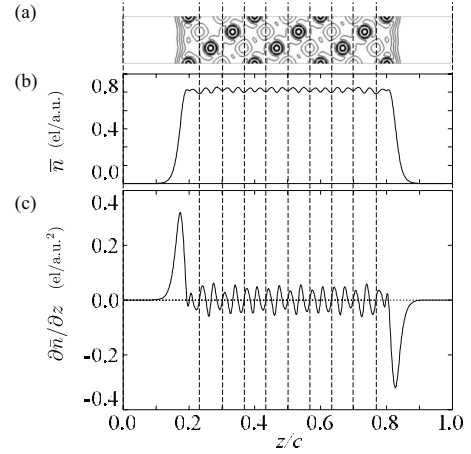


FIG. 2. (a) Contour plots of the valence electron density in the ten-layer slab of the Al (111) surface; (b) planar-integrated valence electron-density distribution; and (c) flux distribution of the valence electron density. Vertical broken lines represent the partitioning planes. A horizontal dotted line represents the line where the flux is zero.

supercells. The cutoff energy for the valence wave function was set to 544 eV in all the calculations. These conditions can provide a well-converged total energy within 1 meV/atom. The lattice parameter of the bulk fcc Al was optimized by using the conventional cell, resulting in 4.033 Å [the experimental value of 4.05 Å (Ref. 44)], which is used for the x - y dimensions of the slab supercell. The thickness of a vacuum region was set to be more than 13.97 Å. The atomic positions were relaxed in z direction and the maximum Hellmann-Feynman force was converged to less than 2.6×10^{-3} eV/Å.

For the local stress calculation of the Al (111) surface slab, the flux of the electron density is calculated after obtaining the stable atomic and electronic structures as shown in Fig. 2. The partitioning planes are determined so as to satisfy the conditions of Eq. (23) and to include atomic spheres inside each region. The stress density $\tau_{\alpha\beta}$ is integrated over each region. First, the density is integrated in the x - y planes, where first-order Newton-Cotes integration scheme is employed. This is accurate enough because the error of numerical integration is canceled due to its periodicity in the x and y directions. Then the planar-integrated stress is integrated along z axis over each partial region. This integration along z axis requires higher-order numerical accuracy due to arbitrary positions of the partitioning planes and we use Gauss-Legendre numerical scheme with six-order interpolation. Finally we obtain the layer-by-layer stress via dividing the integrated value by the volume of each partial region as Eq. (3). Alternatively, we express the local stress by the gross integrated value in each region without the division by V_i , so as to prevent the effects of ambiguous definition of the volume of the top surface region. Thus the layer-by-layer stress is expressed in unit of eV/AL in a similar way to Ref. 29.

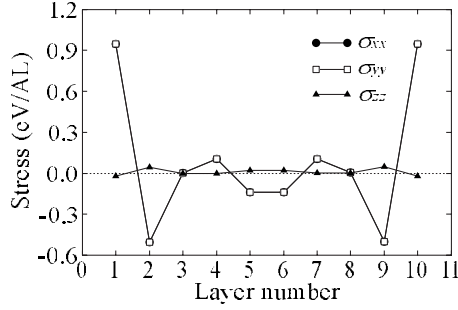


FIG. 3. Layer-by-layer stress distribution for the ten-layer slab of the Al (111) surface. Lines are a guide for the eyes. σ_{xx} and σ_{yy} reveal the same distribution, indicating the isotropic in-plane stress.

III. RESULTS AND DISCUSSION

A. Al fcc (111) surface with ten layers

Figure 3 shows the layer-by-layer stress obtained by the present scheme. As discussed in the previous section, σ_{zz} is only a gauge-dependent component. The kinetic gauge-dependent component in Eq. (16) integrated to be vanishingly small, 10^{-7} eV/AL for σ_{zz} in each region, indicating that the partitioning planes are properly set. Because of the free atomic relaxation along z axis, σ_{zz} for each layer is nearly zero. The distributions of σ_{xx} and σ_{yy} are identical, which means that the layer-by-layer stress parallel to the surface is isotropic due to the hexagonal symmetry of the Al (111) plane.³² We found layer-by-layer oscillating behavior in σ_{xx} and σ_{yy} as reported by Feibelman.³⁰ In Fig. 4, we compare the in-plane layer-by-layer stress obtained in the nine-layer slab with the results of Ref. 29. The agreement is rather good in spite of different DFT functionals (LDA in Ref. 29) and different lattice constants. In Ref. 29, the contributions to the strain derivative of the total energy are obtained as decomposed into the contribution at each atomic layer by using the local atomic-orbital basis scheme. The present scheme has more generality and accuracy than the scheme of Ref. 29. The latter is restricted to the local atomic-orbital basis while our scheme can be implemented by any basis functions basically. The plane-wave basis is superior to the local atomic-orbital basis in accuracy in dealing with metallic surfaces or interfaces if the cutoff energy is large enough.⁴⁵ Although the distributions in the top and second layers are very similar in Fig. 4, the distributions in the

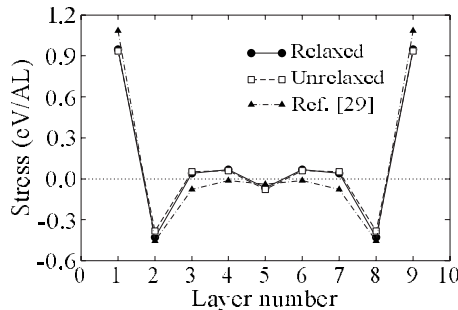


FIG. 4. In-plane layer-by-layer stress distribution for the nine-layer slab of the Al (111) surface. Lines are a guide for the eyes.

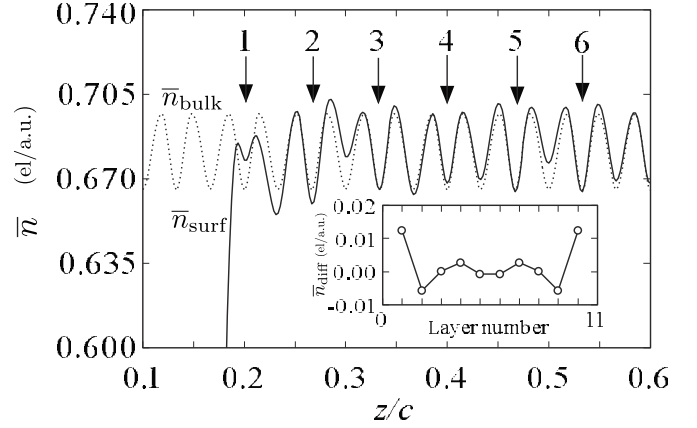


FIG. 5. Planar-integrated valence electron-density distribution of the ten-layer Al (111) surface slab \bar{n}_{surf} and the bulk \bar{n}_{bulk} (outer panel). The difference between the two densities $\bar{n}_{\text{diff}} = \bar{n}_{\text{surf}} - \bar{n}_{\text{bulk}}$ at the atomic-layer positions is plotted in the inner panel. The arrows with numbers indicate the atomic-layer positions.

middle layers are apparently different: the layer-by-layer stress obtained in the present study is still oscillating even in the middle layer. It was reported that the atomic relaxation gives up to 0.5% expansion of the interlayer spacing between the middle layers.⁴⁶ Nevertheless, the comparison of the layer-by-layer stress between the relaxed and unrelaxed surfaces shown in Fig. 4 indicates that the layer-by-layer stress oscillation in the middle layers does not come from this expansion of the interlayer spacing. While the stress behavior inside a surface cannot be experimentally observed, this oscillation can be reasonably explained as follows. The fcc Al is reported as a simple metal with rather free-electronlike features,³² thus we can expect a simple correlation between stress and charge redistribution at the surface.^{8,10} For each Al atom on the (111) plane, six first neighbors out of 12 first neighbors are located on the same (111) plane and thus the charge redistribution on each (111) atomic plane greatly affects the strength of in-plane bonds. Then the variation in the bonding strength should result in the layer-by-layer stress distribution. Figure 5 shows the difference in the planar-integrated electron density between the ten-layer surface slab and the Al bulk. The distribution of the layer-by-layer in-plane stress in Fig. 3 reveals the apparent resemblance with the distribution of the difference of the planar-integrated charge at the atomic-plane positions shown in the inner panel of Fig. 5. The oscillation of the charge at the atomic plane indeed exists beyond the third layer from the surface.

Figure 6 shows the valence electron-density redistributions on the top and second layers of the ten-layer slab. The significant charge increase at the top (111) plane is caused by the less coordination, which is consistent with previous *ab initio* results revealing remarkable charge redistribution at less-coordinated atoms around point defects, surfaces, and grain boundaries in Al.⁴⁷⁻⁵⁰ This should be general nature of Al with high density of s and p electrons. Then there occurs the remarkable charge decrease at the second (111) plane and the oscillation inside the slab occurs as general Friedel-type behavior of metallic electrons. The strengthening and weakening of the in-plane bonds, caused by the in-plane charge-

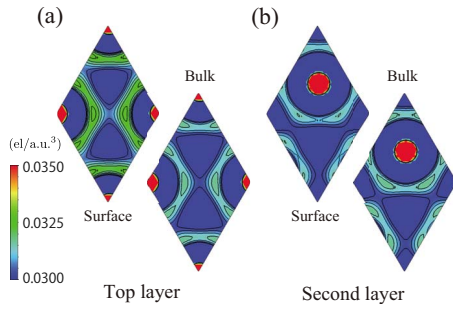


FIG. 6. (Color online) Valence electron-density distributions on (a) the top atomic layer and (b) the second atomic layer in the ten-layer Al (111) surface slab. Distributions on the corresponding layers of the Al bulk are also shown for comparison. The magnitude of the density is expressed by in the color (or gray) scale and the contour so that the bonding charge can be observed.

density variation, induce in-plane tensile stress and in-plane compressive stress, respectively. The change in the in-plane bond strength cannot change the in-plane interatomic bond lengths at the surface due to the constraint of the crystal structure, resulting in the in-plane stress variations.⁸ It is quite interesting to see that the peculiar charge redistribution and oscillation at the Al surface directly induces peculiar stress distribution, which can be easily clarified by the present scheme.

B. Al fcc (111) surface with 9–17 layers

The present results indicate that enough thick slabs are necessary to obtain well-converged surface properties. Furthermore, thin slabs may induce quantum-well states, which seemed to affect the averaged surface stress depending on the slab thickness as observed in Mo thin films.⁵¹ By calculating the layer-by-layer stress, one can easily know how (and how far) the stress variation exists inside a surface. Figure 7 shows the results of the layer-by-layer stress calculations with different slab thickness. In all cases, σ_{zz} is nearly zero, the in-plane stress is isotropic, and the in-plane layer-by-layer stress reveals oscillatory reduction from the surface layer to the slab center. In Ref. 46, the calculated properties of the Al (111) surface such as surface energies, work functions, interlayer relaxations, and the densities of states at the Fermi level clearly reveal the oscillation against the slab thickness. This is obviously attributed to a Friedel-type effect in the vicinity of the surface.⁵² Even in the case of the 17-layer slab, σ_{xx} and σ_{yy} are still oscillating at the slab center. It seems that the Friedel-type effect induced by the surface extends to a depth of more than eight layers, indicating the necessary slab thickness for correct surface calculations.

IV. CONCLUSION

A practical scheme to calculate local quantum stress within the framework of the stress density developed by Filippetti and Fiorentini was described. The gauge-dependent terms and related ambiguities in the stress density were specified, and the conditions were given for defining the local regions where the local stress components are uniquely

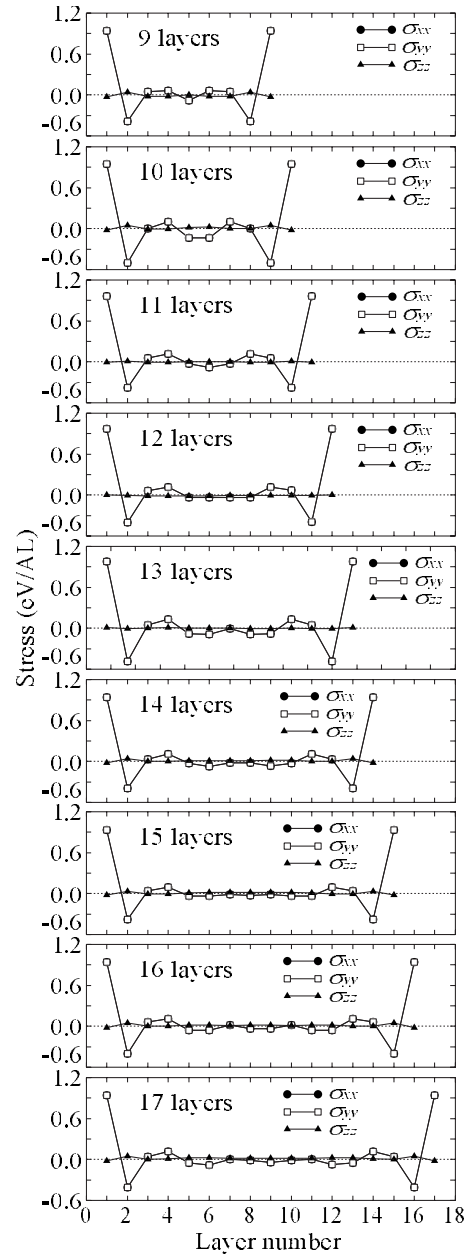


FIG. 7. Layer-by-layer stress distributions for the Al (111) surface slabs with 9–17 layers. Lines are a guide for the eyes. In every case, σ_{xx} and σ_{yy} are equal. The layer-by-layer stress shows oscillatory reduction toward the center of the slab.

obtained. The layer-by-layer stress of the Al (111) surface calculated by the present scheme is physically valid, reflecting the variation in atomic bonding caused by the remarkable charge redistribution and oscillation at the surface. The long-range oscillatory reduction in the surface stress indicates the necessity of enough slab thickness in surface calculations. To apply the present scheme to wide-ranged systems, we have to investigate the numerical techniques to define general three-dimensional integration regions and to perform the stress-density integration in such regions, in contrast to rather simple one-dimensional integration of the present example. In spite of such difficulties, the present scheme is a promising tool to deal with stress-mediated phenomena or

local mechanical properties of defects, surfaces, interfaces, and nanostructures from the behavior of valence electrons.⁵³

ACKNOWLEDGMENTS

This work was partly supported by Next Generation Super-Computing Project, MEXT, Japan. We are grateful to T. Tamura, S. Tanaka, and K. Terakura for helpful comments and discussions.

APPENDIX A: PROOF OF EQS. (8) and (16)

Equation (8) on the relation between the symmetric and asymmetric forms of the kinetic-energy density is proved as follows: $\nabla^2 \rho_e(\mathbf{r})$ in Eq. (8) is expressed as

$$\begin{aligned} \nabla^2 \rho_e(\mathbf{r}) &= \sum_i f_i \nabla^2 [\psi_i^*(\mathbf{r}) \psi_i(\mathbf{r})] = \sum_i f_i \left\{ \frac{\partial^2}{\partial x^2} [\psi_i^*(\mathbf{r}) \psi_i(\mathbf{r})] \right. \\ &\quad \left. + \frac{\partial^2}{\partial y^2} [\psi_i^*(\mathbf{r}) \psi_i(\mathbf{r})] + \frac{\partial^2}{\partial z^2} [\psi_i^*(\mathbf{r}) \psi_i(\mathbf{r})] \right\}, \quad (\text{A1}) \end{aligned}$$

where f_i is the occupancy of an eigenstate ψ_i . Each term is expressed as

$$\begin{aligned} \frac{\partial^2}{\partial x^2} [\psi_i^*(\mathbf{r}) \psi_i(\mathbf{r})] &= \frac{\partial^2 \psi_i^*(\mathbf{r})}{\partial x^2} \psi_i(\mathbf{r}) + 2 \frac{\partial \psi_i^*(\mathbf{r})}{\partial x} \frac{\partial \psi_i(\mathbf{r})}{\partial x} \\ &\quad + \psi_i^*(\mathbf{r}) \frac{\partial^2 \psi_i(\mathbf{r})}{\partial x^2}. \quad (\text{A2}) \end{aligned}$$

Thus

$$\begin{aligned} \nabla^2 \rho_e(\mathbf{r}) &= \sum_i f_i [\psi_i(\mathbf{r}) \nabla^2 \psi_i^*(\mathbf{r}) + 2 \nabla \psi_i^*(\mathbf{r}) \cdot \nabla \psi_i(\mathbf{r}) \\ &\quad + \psi_i^*(\mathbf{r}) \nabla^2 \psi_i(\mathbf{r})] = 2 \sum_i f_i [\nabla \psi_i^*(\mathbf{r}) \cdot \nabla \psi_i(\mathbf{r}) \\ &\quad + \psi_i^*(\mathbf{r}) \nabla^2 \psi_i(\mathbf{r})]. \quad (\text{A3}) \end{aligned}$$

Here we used the theorem that both ψ_i and ψ_i^* are the eigenstates with the same energy and occupancy by the time-reversal symmetry. By Eq. (A3), we get the final relation as

$$-\frac{1}{2} \sum_i f_i \psi_i^*(\mathbf{r}) \nabla^2 \psi_i(\mathbf{r}) = \frac{1}{2} \sum_i f_i \nabla \psi_i^*(\mathbf{r}) \cdot \nabla \psi_i(\mathbf{r}) - \frac{1}{4} \nabla^2 \rho_e(\mathbf{r}). \quad (\text{A4})$$

If we start from the left-hand side of Eq. (A4), the right-hand side can be also obtained via Green's theorem and Gauss's theorem as argued in an early paper of Slater.³⁴ The second term of the right-hand side is the gauge-dependent term causing the indefinite nature.

In order to prove Eq. (16), we use the following equation:

$$\begin{aligned} \nabla_\alpha \nabla_\beta \rho_e(\mathbf{r}) &= \sum_i f_i \frac{\partial^2}{\partial r_\alpha \partial r_\beta} [\psi_i^*(\mathbf{r}) \psi_i(\mathbf{r})] \\ &= \sum_i f_i \left[\frac{\partial^2 \psi_i^*(\mathbf{r})}{\partial r_\alpha \partial r_\beta} \psi_i(\mathbf{r}) + \frac{\partial \psi_i^*(\mathbf{r})}{\partial r_\alpha} \frac{\partial \psi_i(\mathbf{r})}{\partial r_\beta} \right. \\ &\quad \left. + \frac{\partial \psi_i^*(\mathbf{r})}{\partial r_\beta} \frac{\partial \psi_i(\mathbf{r})}{\partial r_\alpha} + \psi_i^*(\mathbf{r}) \frac{\partial^2 \psi_i(\mathbf{r})}{\partial r_\alpha \partial r_\beta} \right] \end{aligned}$$

$$\begin{aligned} &= \sum_i f_i \left[2 \psi_i^*(\mathbf{r}) \frac{\partial^2 \psi_i(\mathbf{r})}{\partial r_\alpha \partial r_\beta} + 2 \frac{\partial \psi_i^*(\mathbf{r})}{\partial r_\alpha} \frac{\partial \psi_i(\mathbf{r})}{\partial r_\beta} \right] \\ &= 2 \sum_i f_i [\psi_i^*(\mathbf{r}) \nabla_\alpha \nabla_\beta \psi_i(\mathbf{r}) + \nabla_\alpha \psi_i^*(\mathbf{r}) \nabla_\beta \psi_i(\mathbf{r})]. \quad (\text{A5}) \end{aligned}$$

In the third line, we used the theorem that both ψ_i and ψ_i^* are the eigenstates with the same energy and occupancy by the time-reversal symmetry. The following relation between the symmetric and asymmetric forms of the kinetic stress density is obtained by rewriting Eq. (A5):

$$\begin{aligned} \sum_i f_i \psi_i^*(\mathbf{r}) \nabla_\alpha \nabla_\beta \psi_i(\mathbf{r}) &= - \sum_i f_i \nabla_\alpha \psi_i^*(\mathbf{r}) \nabla_\beta \psi_i(\mathbf{r}) \\ &\quad + \frac{1}{2} \nabla_\alpha \nabla_\beta \rho_e(\mathbf{r}). \quad (\text{A6}) \end{aligned}$$

The second term in Eq. (A6) is the gauge-dependent term, which is expressed generally using the parameter γ in Eq. (16) similarly to Eq. (8).

Then we derive the expression of the kinetic stress density in Eq. (A6) from the kinetic-energy density in Eq. (A4). The asymmetric kinetic energy is expressed by the integration of the asymmetric kinetic-energy density as

$$E_{\text{kin,asy}} = -\frac{1}{2} \sum_i f_i \int \psi_i^*(\mathbf{r}) \nabla^2 \psi_i(\mathbf{r}) d\mathbf{r}. \quad (\text{A7})$$

The stress density is derived by the scaling procedure given in the works of Nielsen and Martin.^{14,15} The energy of the system with infinitesimal homogeneous strain is given as

$$\begin{aligned} E_{\text{kin,asy}}^e &= -\frac{1}{2} \sum_i f_i \int \psi_i^e(\mathbf{r}') \nabla'^2 \psi_i^e(\mathbf{r}') d\mathbf{r}' \\ &= -\frac{1}{2} \sum_i f_i \int \left(1 - \sum_\alpha \varepsilon_{\alpha\alpha} \right) \psi_i^*(\mathbf{r}) \\ &\quad \times \left(\nabla^2 - 2 \sum_{\alpha\beta} \varepsilon_{\alpha\beta} \nabla_\alpha \nabla_\beta \right) \psi_i(\mathbf{r}) \left(1 + \sum_\alpha \varepsilon_{\alpha\alpha} \right) d\mathbf{r} \\ &\approx -\frac{1}{2} \sum_i f_i \int \psi_i^*(\mathbf{r}) \\ &\quad \times \left(\nabla^2 - 2 \sum_{\alpha\beta} \varepsilon_{\alpha\beta} \nabla_\alpha \nabla_\beta \right) \psi_i(\mathbf{r}) d\mathbf{r}, \quad (\text{A8}) \end{aligned}$$

where the following relations¹⁴ as

$$\mathbf{r}' = (\mathbf{I} + \boldsymbol{\varepsilon}) \cdot \mathbf{r},$$

$$\psi_i^e(\mathbf{r}') = \det|\mathbf{I} + \boldsymbol{\varepsilon}|^{-1/2} \psi_i(\mathbf{r}),$$

$$\det|\mathbf{I} + \boldsymbol{\varepsilon}|^{\pm 1} \approx 1 \pm \sum_\alpha \varepsilon_{\alpha\alpha}$$

are used. Then the derivative of the kinetic energy by the strain tensor is given as a remaining first-order coefficient of the strain tensor in the expansion of Eq. (A8) as

$$\frac{\partial E_{\text{kin,asy}}}{\partial \varepsilon_{\alpha\beta}} \equiv \lim_{\varepsilon \rightarrow 0} \frac{\partial E_{\text{kin,asy}}^{\varepsilon}}{\partial \varepsilon_{\alpha\beta}} = \sum_i f_i \int \psi_i^*(\mathbf{r}) \nabla_{\alpha} \nabla_{\beta} \psi_i(\mathbf{r}) d\mathbf{r}. \quad (\text{A9})$$

The final form of Eq. (A9) shows that the left-hand side of Eq. (A6) is indeed the asymmetric kinetic stress density.

For the symmetric kinetic stress density from the symmetric kinetic-energy density, we consider the strained symmetric kinetic energy as

$$\begin{aligned} E_{\text{kin,sym}}^{\varepsilon} &= \frac{1}{2} \sum_i f_i \int \nabla' \psi_i^*(\mathbf{r}') \cdot \nabla' \psi_i(\mathbf{r}') d\mathbf{r}' \\ &\approx \frac{1}{2} \sum_i f_i \int \left(1 - \sum_{\alpha} \varepsilon_{\alpha\alpha} \right) \left[\nabla \psi_i^*(\mathbf{r}) \cdot \nabla \psi_i(\mathbf{r}) \right. \\ &\quad \left. - 2 \sum_{\alpha\beta} \varepsilon_{\alpha\beta} \nabla_{\alpha} \psi_i^*(\mathbf{r}) \nabla_{\beta} \psi_i(\mathbf{r}) \right] \left(1 + \sum_{\alpha} \varepsilon_{\alpha\alpha} \right) d\mathbf{r} \\ &\approx \frac{1}{2} \sum_i f_i \int \left[\nabla \psi_i^*(\mathbf{r}) \cdot \nabla \psi_i(\mathbf{r}) \right. \\ &\quad \left. - 2 \sum_{\alpha\beta} \varepsilon_{\alpha\beta} \nabla_{\alpha} \psi_i^*(\mathbf{r}) \nabla_{\beta} \psi_i(\mathbf{r}) \right] d\mathbf{r}. \end{aligned} \quad (\text{A10})$$

In a similar way to Eq. (A9), the strain derivative of the energy is obtained as

$$\frac{\partial E_{\text{kin,sym}}}{\partial \varepsilon_{\alpha\beta}} = - \sum_i f_i \int \nabla_{\alpha} \psi_i^*(\mathbf{r}) \nabla_{\beta} \psi_i(\mathbf{r}) d\mathbf{r}. \quad (\text{A11})$$

The final form indicates the symmetric kinetic stress as the right-hand side of Eq. (A6).

In addition, the relation between the second term of the right-hand side of Eq. (A6) and that of Eq. (A4) can be explained as follows. The strained energy component of the Laplacian of the electron density in Eq. (A4) is given as

$$\begin{aligned} \left[-\frac{1}{4} \int \nabla^2 \rho_e(\mathbf{r}) d\mathbf{r} \right]^{\varepsilon} &= -\frac{1}{4} \int \nabla'^2 \rho_e^{\varepsilon}(\mathbf{r}') d\mathbf{r}' \\ &= -\frac{1}{4} \int \left(\nabla^2 - 2 \sum_{\alpha\beta} \varepsilon_{\alpha\beta} \frac{\partial}{\partial r_{\alpha}} \frac{\partial}{\partial r_{\beta}} \right) \\ &\quad \times \left(1 - \sum_{\alpha} \varepsilon_{\alpha\alpha} \right) \rho_e(\mathbf{r}) \left(1 + \sum_{\alpha} \varepsilon_{\alpha\alpha} \right) d\mathbf{r} \\ &\approx -\frac{1}{4} \int \left(\nabla^2 - 2 \sum_{\alpha\beta} \varepsilon_{\alpha\beta} \nabla_{\alpha} \nabla_{\beta} \right) \rho_e(\mathbf{r}) d\mathbf{r}, \end{aligned} \quad (\text{A12})$$

where the strained charge density¹⁴

$$\rho_e^{\varepsilon}(\mathbf{r}') = \det[\mathbf{I} + \varepsilon]^{-1} \rho_e(\mathbf{r}) \quad (\text{A13})$$

is introduced. Then its strain derivative is given as

$$\frac{\partial}{\partial \varepsilon_{\alpha\beta}} \left(-\frac{1}{4} \int \nabla^2 \rho_e(\mathbf{r}) d\mathbf{r} \right) = \frac{1}{2} \int \nabla_{\alpha} \nabla_{\beta} \rho_e(\mathbf{r}) d\mathbf{r}. \quad (\text{A14})$$

This expression is equivalent to the second term of the right-hand side of the Eq. (A6).

APPENDIX B: EXCHANGE-CORRELATION STRESS DENSITY

The exchange-correlation stress density is derived from the exchange-correlation energy density $e_{\text{xc}}(\mathbf{r}) = e_{\text{xc}}[\rho_e(\mathbf{r}), \nabla \rho_e(\mathbf{r})]$ as a functional of the electron density and its gradient in GGA. The exchange-correlation energy per supercell is

$$E_{\text{xc}} = \int e_{\text{xc}}[\rho_e(\mathbf{r}), \nabla \rho_e(\mathbf{r})] \rho_e(\mathbf{r}) d\mathbf{r}. \quad (\text{B1})$$

The strained exchange-correlation energy is obtained in a similar way in Appendix A,

$$\begin{aligned} E_{\text{xc}}^{\varepsilon} &= \int e_{\text{xc}}^{\varepsilon}(\mathbf{r}') d\mathbf{r}' = \int \left[e_{\text{xc}}(\mathbf{r}) + \sum_{\alpha\beta} \varepsilon_{\alpha\beta} \left(\frac{\partial e_{\text{xc}}}{\partial \rho_e} \frac{\partial \rho_e}{\partial \varepsilon_{\alpha\beta}} \right. \right. \\ &\quad \left. \left. + \frac{\partial e_{\text{xc}}}{\partial \nabla \rho_e} \cdot \frac{\partial \nabla \rho_e}{\partial \varepsilon_{\alpha\beta}} \right) \right] \left(1 + \sum_{\alpha} \varepsilon_{\alpha\alpha} \right) d\mathbf{r} = \int \left[e_{\text{xc}}(\mathbf{r}) \right. \\ &\quad \left. + \sum_{\alpha} \varepsilon_{\alpha\alpha} e_{\text{xc}}(\mathbf{r}) + \sum_{\alpha\beta} \varepsilon_{\alpha\beta} \left(\frac{\partial e_{\text{xc}}}{\partial \rho_e} \frac{\partial \rho_e}{\partial \varepsilon_{\alpha\beta}} + \frac{\partial e_{\text{xc}}}{\partial \nabla \rho_e} \cdot \frac{\partial \nabla \rho_e}{\partial \varepsilon_{\alpha\beta}} \right) \right] d\mathbf{r}. \end{aligned} \quad (\text{B2})$$

Then its strain derivative is

$$\frac{\partial E_{\text{xc}}}{\partial \varepsilon_{\alpha\beta}} = \int \left[\delta_{\alpha\beta} e_{\text{xc}}(\mathbf{r}) + \frac{\partial e_{\text{xc}}}{\partial \rho_e} \frac{\partial \rho_e}{\partial \varepsilon_{\alpha\beta}} + \frac{\partial e_{\text{xc}}}{\partial \nabla \rho_e} \cdot \frac{\partial \nabla \rho_e}{\partial \varepsilon_{\alpha\beta}} \right] d\mathbf{r}. \quad (\text{B3})$$

In the case of LDA, the last term of Eq. (B3) vanishes. Then we obtain

$$\frac{\partial E_{\text{xc}}^{\text{LDA}}}{\partial \varepsilon_{\alpha\beta}} = \int \delta_{\alpha\beta} \left[e_{\text{xc}}(\mathbf{r}) - \rho_e(\mathbf{r}) \frac{\partial e_{\text{xc}}}{\partial \rho_e} \right] d\mathbf{r}. \quad (\text{B4})$$

The form of Eq. (B4) is identical to that in Refs. 14 and 15. For the strained forms of electron density and its gradient, the compensation charge and core-correction charge have to be dealt with in the PAW scheme. We have to add the contributions of such components, which is practically easily attained by using the expression in the reciprocal space.

APPENDIX C: PAW EXPRESSIONS OF NONLOCAL PSEUDOPOTENTIAL TERMS IN THE ENERGY DENSITY AND STRESS DENSITY

In this paper, all the terms in the energy and stress densities are expressed by the PAW scheme in contrast to the norm-conserving pseudopotential (NCP) method for the energy density in Ref. 16 and the USPP method for the stress density in Ref. 15. The PAW expressions of the kinetic, electrostatic, and exchange-correlation terms have similar features to those by the USPP or NCP schemes while the PAW expressions of the nonlocal pseudopotential terms concerning Eqs. (13), (14), and (18) are rather different from those by the other schemes. Here we show the summary of the PAW expressions of the nonlocal pseudopotential terms. We use the PAW formulation and terms similar to those in Ref.

27. The nonlocal pseudopotential term in the energy density is expressed as

$$e_{nl}(\mathbf{r}) = \sum_a \delta(\mathbf{r} - \mathbf{R}_a) (E_a^1 - \tilde{E}_a^1). \quad (\text{C1})$$

E_a^1 and \tilde{E}_a^1 are the total-energy terms inside the atomic radius of the atom a at the site \mathbf{R}_a , expressed by the all-electron (AE) partial waves ϕ_i^a and the on-site AE valence and core charge densities $n_a^1 + n_c^a$, and expressed by the pseudo (PS) partial waves $\{\tilde{\phi}_i^a\}$ and the on-site PS valence and compensation charge densities $\tilde{n}_a^1 + \hat{n}_a$ with the partial core charge \tilde{n}_c^a , respectively. $E_a^1 - \tilde{E}_a^1$ is given as

$$\begin{aligned} E_a^1 - \tilde{E}_a^1 = & \sum_{ij} \rho_{ij}^a \langle \phi_i^a | -\frac{1}{2} \Delta | \phi_j^a \rangle + \overline{E_H[n_a^1]} + \int_{\Omega_a} v_H[n_{zc}] n_a^1 d\mathbf{r} \\ & + \overline{E_{xc}[n_a^1 + n_c^a]} - \sum_{ij} \rho_{ij}^a \langle \tilde{\phi}_i^a | -\frac{1}{2} \Delta | \tilde{\phi}_j^a \rangle - \overline{E_H[\tilde{n}_a^1 + \hat{n}_a]} \\ & - \int_{\Omega_a} v_{loc}^a(r) (\tilde{n}_a^1 + \hat{n}_a) d\mathbf{r} - \overline{E_{xc}[\tilde{n}_a^1 + \hat{n}_a + \tilde{n}_c^a]}. \quad (\text{C2}) \end{aligned}$$

ρ_{ij}^a is the occupancy of the augmentation channel (i, j) at the atomic site obtained by the projectors $\{\tilde{p}_i^a\}$ and the extended pseudowave functions $\{\tilde{\psi}_{\mathbf{k}n}\}$ as

$$\rho_{ij}^a = \sum_{\mathbf{k}n} f_{\mathbf{k}n} \langle \tilde{\psi}_{\mathbf{k}n} | \tilde{p}_i^a \rangle \langle \tilde{p}_j^a | \tilde{\psi}_{\mathbf{k}n} \rangle. \quad (\text{C3})$$

The AE and PS on-site charge densities are given by

$$n_a^1(\mathbf{r}) = \sum_{ij} \rho_{ij}^a \phi_i^{a*}(\mathbf{r}) \phi_j^a(\mathbf{r}) \quad (\text{C4})$$

and

$$\tilde{n}_a^1(\mathbf{r}) = \sum_{ij} \rho_{ij}^a \tilde{\phi}_i^{a*}(\mathbf{r}) \tilde{\phi}_j^a(\mathbf{r}). \quad (\text{C5})$$

The compensation charge density \hat{n}_a at the atomic site is given by

$$\hat{n}_a(\mathbf{r}) = \sum_{ij} \rho_{ij}^a \sum_{lm} \hat{Q}_{ij,a}^{lm}(\mathbf{r}), \quad (\text{C6})$$

where

$$\hat{Q}_{ij,a}^{lm}(\mathbf{r}) = q_{ij,a}^{lm} g_i^a(r) Y_{lm}(\hat{r}). \quad (\text{C7})$$

$q_{ij,a}^{lm}$ is the moment of $Q_{ij}^a(\mathbf{r})$, which is the charge-density difference between the AE and PS partial waves for an (i, j) channel within the augmentation region, expressed as $Q_{ij}^a(\mathbf{r}) = \phi_i^{a*}(\mathbf{r}) \phi_j^a(\mathbf{r}) - \tilde{\phi}_i^{a*}(\mathbf{r}) \tilde{\phi}_j^a(\mathbf{r})$. g_i^a is the compensation function of the atom a to smoothen the compensation charge. In this way, \hat{n}_a reproduces the correct moments of $n_a^1 - \tilde{n}_a^1 = \sum_{ij} \rho_{ij}^a Q_{ij}^a(\mathbf{r})$. In Eq. (C2), $\overline{E_H[n]}$ and $\overline{E_{xc}[n]}$ are the electrostatic and exchange-correlation energies for the on-site charge distribution and the bar above each term means that the integration is performed inside the atomic radius by the radial grid. $v_H[n_{zc}]$ and $v_{loc}^a(r)$ are the electrostatic potential from the nuclear and core charge and the unscreened atomic local pseudopotential, respectively. The integration is also performed inside the atomic radius (the sphere Ω_a).

The nonlocal pseudopotential term in the stress density is given as

$$\tau_{nl,\alpha\beta}(\mathbf{r}) = \sum_a \delta(\mathbf{r} - \mathbf{R}_a) \sum_{ij} \left(\frac{\partial \rho_{ij}^a}{\partial \varepsilon_{\alpha\beta}} \right) (D_{ij,a}^1 - \tilde{D}_{ij,a}^1), \quad (\text{C8})$$

where

$$\begin{aligned} D_{ij,a}^1 = & \langle \phi_i^a | -\frac{1}{2} \nabla^2 | \phi_j^a \rangle + \langle \phi_i^a | v_H[n_{zc}] | \phi_j^a \rangle + \langle \phi_i^a | v_H[n_a^1] | \phi_j^a \rangle \\ & + \langle \phi_i^a | v_{xc}[n_a^1 + n_c^a] | \phi_j^a \rangle \quad (\text{C9}) \end{aligned}$$

and

$$\begin{aligned} \tilde{D}_{ij,a}^1 = & \langle \tilde{\phi}_i^a | -\frac{1}{2} \Delta | \tilde{\phi}_j^a \rangle + \langle \tilde{\phi}_i^a | v_{loc}^a | \tilde{\phi}_j^a \rangle + \langle \tilde{\phi}_i^a | v_H[\tilde{n}_a^1 + \hat{n}_a] | \tilde{\phi}_j^a \rangle \\ & + \langle \tilde{\phi}_i^a | v_{xc}[\tilde{n}_a^1 + \hat{n}_a + \tilde{n}_c^a] | \tilde{\phi}_j^a \rangle + \int_{\Omega_a} (v_{loc}^a + v_H[\tilde{n}_a^1 + \hat{n}_a] \\ & + v_{xc}[\tilde{n}_a^1 + \hat{n}_a + \tilde{n}_c^a]) \times \sum_{lm} \hat{Q}_{ij,a}^{lm}(\mathbf{r}) d\mathbf{r}. \quad (\text{C10}) \end{aligned}$$

$D_{ij,a}^1$ and $\tilde{D}_{ij,a}^1$ are identical to those to appear in the Hamiltonian.²⁸ All the integrations are performed inside the atomic radius. $v_H[n]$ and $v_{xc}[n]$ are the electrostatic and exchange-correlation potentials by the on-site charge distribution n . The term $\frac{\partial \rho_{ij}^a}{\partial \varepsilon_{\alpha\beta}}$ is given in the reciprocal space.

*y.shiuhara@aist.go.jp

¹G. H. Olsen, C. J. Nuese, and R. T. Smith, J. Appl. Phys. **49**, 5523 (1978).

²C. P. Kuo, S. K. Vong, R. M. Cohen, and G. B. Stringfellow, J. Appl. Phys. **57**, 5428 (1985).

³K. Kim, W. R. L. Lambrecht, and B. Segall, Phys. Rev. B **50**, 1502 (1994).

⁴Y. Suzuki, H. Y. Hwang, S. W. Cheong, and R. B. van Dover, Appl. Phys. Lett. **71**, 140 (1997).

⁵T. K. Nath, R. A. Rao, D. Lavric, C. B. Eom, L. Wu, and F. Tsui, Appl. Phys. Lett. **74**, 1615 (1999).

⁶L. A. Knauss, X. M. Wang, and J. Toulouse, Phys. Rev. B **52**, 13261 (1995).

⁷S. E. Park and T. R. Shrout, J. Appl. Phys. **82**, 1804 (1997).

⁸H. Ibach, Surf. Sci. Rep. **29**, 195 (1997).

⁹M. Hanbücken and J. P. Deville, *Stress and Strain in Epitaxy: Theoretical Concepts, Measurements and Applications* (Elsevier, Amsterdam, 2001).

¹⁰W. Haiss, Rep. Prog. Phys. **64**, 591 (2001).

¹¹K. O. Schweitz, J. Böttiger, J. Chevallier, R. Feidenhans'l, N. M. Nielsen, and F. B. Rasmussen, J. Appl. Phys. **88**, 1401 (2000).

¹²R. Birringer, M. Hoffmann, and P. Zimmer, Phys. Rev. Lett. **88**,

- 206104 (2002).
- ¹³R. Maranganti, P. Sharma, and L. Wheeler, *J. Aerosp. Eng.* **20**, 22 (2007).
- ¹⁴O. H. Nielsen and R. M. Martin, *Phys. Rev. B* **32**, 3780 (1985).
- ¹⁵O. H. Nielsen and R. M. Martin, *Phys. Rev. B* **32**, 3792 (1985).
- ¹⁶A. Filippetti and V. Fiorentini, *Phys. Rev. B* **61**, 8433 (2000).
- ¹⁷N. Chetty and R. M. Martin, *Phys. Rev. B* **45**, 6074 (1992).
- ¹⁸N. O. Folland, *Phys. Rev. B* **34**, 8296 (1986).
- ¹⁹M. J. Godfrey, *Phys. Rev. B* **37**, 10176 (1988).
- ²⁰Y. A. Uspenskii, P. Ziesche, and J. Gräfenstein, *Z. Phys. B: Condens. Matter* **76**, 193 (1989).
- ²¹C. L. Rogers and A. M. Rappe, *Phys. Rev. B* **65**, 224117 (2002).
- ²²R. M. Martin, *Electronic Structure: Basic Theory and Practical Methods* (Cambridge University Press, Cambridge, England, 2004).
- ²³A. Baldereschi, S. Baroni, and R. Resta, *Phys. Rev. Lett.* **61**, 734 (1988).
- ²⁴K. Rapcewicz, B. Chen, B. Yakobson, and J. Bernholc, *Phys. Rev. B* **57**, 7281 (1998).
- ²⁵G. B. Bachelet, D. R. Hamann, and M. Schlüter, *Phys. Rev. B* **26**, 4199 (1982).
- ²⁶D. Vanderbilt, *Phys. Rev. B* **41**, 7892 (1990).
- ²⁷P. E. Blöchl, *Phys. Rev. B* **50**, 17953 (1994).
- ²⁸G. Kresse and D. Joubert, *Phys. Rev. B* **59**, 1758 (1999).
- ²⁹S. Ishibashi, T. Tamura, S. Tanaka, M. Kohyama, and K. Terakura, *Phys. Rev. B* **76**, 153310 (2007).
- ³⁰P. J. Feibelman, *Phys. Rev. B* **50**, 1908 (1994).
- ³¹R. J. Needs, *Phys. Rev. Lett.* **58**, 53 (1987).
- ³²R. J. Needs and M. J. Godfrey, *Phys. Rev. B* **42**, 10933 (1990).
- ³³Strictly speaking, $\tau_{\alpha\beta}$ in the present definition should be called as stress field instead of stress density because this does not express the density distribution. Thus the macroscopic stress is given by the volume-average as Eq. (1). However, according to Ref. 15, we use the term of stress density as the same meaning of stress field for simplicity.
- ³⁴J. C. Slater, *Phys. Rev.* **51**, 846 (1937).
- ³⁵Z. Z. Yang, S. Liu, and Y. A. Wang, *Chem. Phys. Lett.* **258**, 30 (1996).
- ³⁶R. P. Feynman, R. B. Leighton, and M. Sands, *The Feynman Lectures on Physics*, The Definitive Edition Vol. 2 (Pearson, Addison-Wesley, San Francisco, 2006), pp. 15.14–15.16.
- ³⁷In ultrasoft pseudopotential method or PAW method, the stress component due to an overlap operator need to be added.
- ³⁸L. D. Landau and E. M. Lifshits, *The Classical Theory of Fields*, 4th revised English edition (Butterworth-Heinemann, London, 2007).
- ³⁹A. Kugler, *Z. Phys.* **198**, 236 (1967).
- ⁴⁰J. Gräfenstein and P. Ziesche, *Phys. Rev. B* **41**, 3245 (1990).
- ⁴¹P. Ziesche, J. Gräfenstein, and O. H. Nielsen, *Phys. Rev. B* **37**, 8167 (1988).
- ⁴²J. P. Perdew, K. Burke, and M. Ernzerhof, *Phys. Rev. Lett.* **77**, 3865 (1996).
- ⁴³C. L. Fu and K. M. Ho, *Phys. Rev. B* **28**, 5480 (1983).
- ⁴⁴N. W. Ashcroft and N. D. Mermin, *Solid State Physics* (Thomson Learning, Singapore, 1976).
- ⁴⁵In addition, the present scheme can uniquely determine such a region V_i in Eq. (3) to define the local stress while the scheme in Ref. 29 uses an ambiguous local region for the exchange-correlation terms coupled with the decomposition of the other energy and stress terms into local atomic-orbital basis. This ambiguity is not a problem when considering the layer-by-layer contribution to the surface stress but it becomes considerably impeditive when one try to develop the local stress scheme aiming for a three-dimensional local stress analysis.
- ⁴⁶J. L. F. Da Silva, *Phys. Rev. B* **71**, 195416 (2005).
- ⁴⁷P. J. Feibelman, *Phys. Rev. Lett.* **65**, 729 (1990).
- ⁴⁸K. Carling, G. Wahnström, T. R. Mattsson, A. E. Mattsson, N. Sandberg, and G. Grimvall, *Phys. Rev. Lett.* **85**, 3862 (2000).
- ⁴⁹T. Uesugi, M. Kohyama, and K. Higashi, *Phys. Rev. B* **68**, 184103 (2003).
- ⁵⁰R. Z. Wang, M. Kohyama, S. Tanaka, T. Tamura, and S. Ishibashi, *Mater. Trans.* **50**, 11 (2009).
- ⁵¹X. Qian and S. R. Wickramasinghe, *J. Phys.: Condens. Matter* **17**, 581 (2005).
- ⁵²F. K. Schulte, *Surf. Sci.* **55**, 427 (1976).
- ⁵³S. Ogata, Y. Umeno, and M. Kohyama, *Modell. Simul. Mater. Sci. Eng.* **17**, 013001 (2008).